RESEARCH ARTICLE

Nanotherapy: New Approach for Impeding Hepatic Cancer Microenvironment *via* Targeting Multiple Molecular Pathways

Ahmed A Abd-Rabou[1,2]*, Hanaa H Ahmed[1,2], Safaa H Mohamed[1], Soheir E Kotob[1], Mohamed S Kishta[1,2]

Abstract

Objective: Hepatocellular carcinoma (HCC) microenvironment has been recognized as a key contributor for cancer progression, metastasis, and drug resistance. The crosstalk between tumor cells, the vascular endothelial growth factor (VEGF), and the chemokine (C-C motif) ligand 2 (CCL2) signaling networks mediates immunoinhibitory impact and facilitates tumor angiogenesis. The current investigation aimed at exploring the potent anti-cancer activity of the newly designed nano-based anti-cancer therapy comprising anti-VEGF drug, avastin (AV), and CCR2 antagonist (CR) to counteract HCC and tracking its mode of action *in vivo*. **Methods:** The prepared AV, CR, and AVCR nanoprototypes were characterized by nanoscale characterization techniques in our previous work. Here, they are applied for unearthing their anti-cancer properties / mechanisms in hepatic cancer-induced rats *via* analyzing protein levels and genetic expression of the elements incorporated in the angiogenesis, apoptosis, and metastasis signalling pathways. **Results:** The present results revealed a significant down-regulation in the angiogenesis, survival and metastasis indices along with up-regulation in the pro-apoptotic mediators upon treatment of hepatic cancer-bearing rats with the novel synthesized nanomaterials when compared with the untreated counterparts. We showed across HCC model that anti-VEGF in combination with CCR2 antagonism therapy leads to sensitization and enhanced tumor response over anti-VEGF or CCR2 antagonism monotherapy, particularly in its nanoscale formulation. **Conclusion:** The present approach provides new mechanistic insights into the powerful anti-hepatic cancer advantage of the novel nanoprototypes which is correlated with modulating critical signal transduction pathways implicated in tumor microenviroment such as angiogenesis, apoptosis and metastasis. This research work presents a substantial foundation for future studies focused on prohibiting cancer progression and recovery by targeting tumor microenviroment.

Keywords: Avastin nanoformulation- CCR2 antagonist nanoprototype- Hepatic cancer microenvironment

Introduction

Tumors are not only formed by the cancer cells themselves; they are rather complex and plastic malignant organs composed of various cell populations. These include tumor vasculature (Farnsworth et al., 2014) and the infiltrating immune cells, such as T lymphocytes (Speiser et al., 2016), B lymphocytes (Tsou et al., 2016), natural killer (NK) cells (Morvan and Lanier, 2016), and tumor-associated macrophages (TAMs) (Baghban et al., 2020).

In the past 15 years, the vascular endothelial growth factor (VEGF) role in the tumor microenvironment has evolved as VEGF is produced from tumor cells and the surrounding stroma (Apte et al., 2019). VEGF not only plays a major role in controlling blood vessel formation, but also modulates tumor-induced immunosuppression (Garcia et al., 2020) *via* VEGFR signaling in hematopoietic

cells (VEGFR1), T cells (VEGFR-1,2), and macrophages (VEGFR1,3) (Rahma and Hodi, 2019).

Hepatocellular carcinoma (HCC) is among the most prevalent and lethal cancers in the human population (Tian et al., 2019). It accounts for 8.2% of all cancer-related deaths worldwide (Alzamzamy et al., 2021). The tumor microenvironment, consisting of immune cells, inflammatory cells, cytokines and extracellular matrix, plays a key role in the initiation and progression of HCC (Hernandez-Gea et al., 2013; Hou et al., 2018). Being a vascular tumor, VEGF plays a vital role in HCC pathogenesis, growth and spread. VEGF is responsible for angiogenesis and it appears to be the most important angiogenic factor in HCC because of the tumor relies on the formation of new blood vessels to grow and spread (Alzamzamy et al., 2021). Several studies report VEGF overexpression in HCC and the higher levels of VEGF in

[1]*Hormones Department, Medicine and Clinical Studies Research Institute, National Research Centre, Cairo, Egypt.* [2]*Stem Cell Lab, Center of Excellence for Advanced Sciences, National Research Centre, Dokki, Giza, P.O 12622, Egypt.* *For Correspondence: ahmedchemia87@yahoo.com*

patients with more advanced stages of the disease (Matsui et al., 2015).

Given the importance of VEGF in tumor biology, drug development efforts in the past decades have been dedicated to targeting VEGF *via* anti-VEGF agents (Ye, 2016). The first available and approved anti-VEGF therapy was Avastin (AV) (F. Hoffmann La-Roche AG, Switzerland). AV has been shown to exhibit anti-tumor properties in many tumors either as a single agent or in combination with other anti-cancer drugs. AV is a humanized monoclonal antibody that, in tumoral tissue, blocks the mechanism that promotes and sustains the new vessel growth (Park et al., 2012). These effects result in induction of cancer apoptosis (Shih and Lindley, 2006).

The development of controlled release systems for AV delivery can promote the modification of drug pharmacokinetics and, consequently, decrease the dose, toxicity, and cost due to improved efficacy (Alves et al., 2021). Therefore, nanocarrier delivery systems that can specifically deliver the drug to the cancer at high concentrations and least toxic to the normal cells have to be developed ((Abd-Rabou et al., 2016; Fekry et al., 2021). These includes the enhanced stability of drug in the systemic circulation, easy modification of particle surface (active targeting), and preferable accumulation in the tumor tissues (Zhang et al., 2015; Swarna latha, 2020).

Chemokines play with their receptors a fundamental role in many pathological process like cancer (Conti and Rollins, 2004; Fang et al., 2012). One of these chemokines is chemokine (C-C motif) ligand 2 (CCL2) which is also known as monocyte chemotactic protein-1 (MCP-1). CCL2 is produced by a variety of activating cells, such as lymphocytes and macrophages (Zachariae et al., 1990) and it was reported that CCL2 participates in monocytes recruitment during angiogenesis (Salcedo et al., 2000). In addition, several reports have mentioned that CCL2 is overexpressed in a majority of solid cancer types, including gastrointestinal cancers (Wolf et al., 2012), resulting in increased recruitment of monocytes into those tumors to destroy the cancer cells (Korbecki et al., 2020). Importantly, CCL2, has been found to facilitate cancer metastasis and the blocking of CCL2/CCR2 signaling by specific inhibitors augments CD8+ T-cell-mediated responses and inhibits the metastatic process (Fridlender et al., 2010; Qian et al., 2011).

The combination of anti-VEGF (AV) with cancer immunotherapy has recently been approved in non-small-cell lung cancer and assign of clinical benefit was also demonstrated for treatment of HCC (Garcia et al., 2020). Treatment of HCC patients with the combination of AV and atezolizumab, a humanized monoclonal antibody immune checkpoint inhibitor resulted in significantly longer overall and progression-free survival as well as strikingly better patient-reported outcomes than sorafenib. This outcome prompts the question of whether their activity in combination reflects additive effects or a synergy resulting from anti-angiogenic immune modulation of the tumor microenvironment (Rahma and Hodi, 2019). Thus, this combination has become the new benchmark for first-line therapy in advanced HCC (Kelley, 2020). In order to achieve this goal, we utilized our previously designed nanoprototypes, AVNPs, CRNPs and named avastin-encapsulated nanoformulation labeled by CCR2 antagonist AVCRNPs, to inhibit angiogenesis and metastasis signaling pathways implicated in the HCC microenvironment and to enhance apoptosis of HCC cells.

Material and Methods

Material
Chemicals and Drugs

Methoxy polyethylene glycol amine (mPEG-NH2, MW 5000 Da), 1-ethyl-3-(3-dimethylaminopropyl)-carbodiimide (EDC), N-hydroxysuccinimide (NHS), heparin, polyethylene glycol (MW 5000 Da), 2-(N morpholine) ethanesulfonic acid (MES), dimethyl sulfoxide (DMSO), Tween 80, and poly L-lysine (PLL), CCR2 antagonist RS 504393: 6-Methyl-1′-[2-(5-methyl-2-phenyl-4-oxazolyl)ethyl]-spiro[4H-3,1-benzoxazine-4,4′-piperidin]-2(1H)-one(CR) and N-nitrosodiethylamine (NDEA) were purchased from Sigma-Aldrich (USA). Avastin (AV) was obtained from (Genentech Inc., USA).

Animals

Adult female albino rats of Wistar strain (3 month old with average body weight of 140 g) were procured from the Animal Care Unit of the National Research Centre, Giza, Egypt. The animals were maintained under strict hygienic conditions in an animal holding room with controlled temperature (22±1 ℃) and humidity (50±10%) as well as regular light/dark illumination cycle (12 h light/dark cycle). The rats were fed with standard laboratory diet consisting of casein 10%, salts mixture 4%, vitamins mixture 1%, corn oil 10% and cellulose 5% completed to 100 g with corn starch (A.O.A.C. 1995) and water ad libitum throughout the course of the experiment. The animals were permitted to adapt to their new environment for one week before the experiment. All the experimental procedures are in accordance with the principles for the management and use of local laboratory animals and approved by the Ethical Committee for Medical Research of the National Research Centre, Egypt under the approval No of 16/281.

Methods
Synthesis of the nanoprototypes

The preparation methods for PEG-exposed nanoparticles [Nano-void (NVNPs)], PEG-nanoparticles of AV monoclonal antibody (AVNPs), PEG-nanoparticles of CCR2 antagonist RS504393 (CRNPs) and AVCRNPs were described in details in our previous work (Abd-Rabou et al., 2019).

Characterization of the synthesized nanoprototypes

The encapsulating (entrapment) efficiency (EE) for the designed nanoprototypes after dialysis was calculated as reported previously in our prior study (Abd-Rabou et al., 2019). Also, particle morphology, by transmission electron microscope (TEM), particle size distribution and zeta potential analysis by Malvern zetasizer were determined for the all synthesized nanoprototypes as indicated in our former research (Abd-Rabou et al., 2019).

Fourier transform infrared spectroscopy (FTIR) spectra of NVNPs, AVNPs, CRNPs and AVCRNPs were estimated as manifested in our past investigation (Abd-Rabou et al., 2019).

In-vivo experiment
Model creation and treatments
Induction of hepatocellular carcinoma (HCC)

HCC model was generated in rats by the fourth week of N-nitrosodiethylamine (NDEA) oral administration at a dose of 20 mg /kg body weight (five times a week) in addition to one week of oral administration of NDEA at a dose of 10 mg/kg body weight (five times a week) (Aglan et al., 2017).

Animal grouping

The rats in this study were classified into nine groups with ten rats in each group as follows: Group (1): This group was set as healthy control group which did not receive any treatment (negative control group (NC)). Group (2): HCC group (positive control group (PC)). Group (3): HCC group treated orally with 0.625 mg/kg body weight of free AV (AV) according to the optimized dose derived from our chronic toxicity study (Mohamed et al., 2019). Group (4): HCC group treated orally with 0.625 mg/kg of AVNPs (AVNPs) according to the optimized dose gained from our chronic toxicity study. Group (5): HCC group treated orally with 0.125 µg/kg of free CR (CR) according to the optimized dose obtained from our chronic toxicity study. Group (6): HCC group treated orally with 0.125 µg/kg of CRNPs (CRNPs) according to the optimized dose acquired from our chronic toxicity study. Group (7): HCC group treated orally with 0.625 mg/kg of free AV and 0.125 µg/kg of CR (AVCR). Group (8): HCC group treated orally with 0.625 mg/kg of AVNPs and 0.125 µg/kg of CRNPs (AVCRNPs). Group (9): HCC group treated orally with doxorubicin (DOX: 0.072 mg/ rat) (DOX) as described in the study of Aglan et al. (2017).

The treatment period lasted for five weeks and at the end of the treatment period (10 weeks), the rats were fasted overnight and subjected to a light anesthesia. The blood samples were immediately withdrawn from the tail vein and sera were separated and cryopreserved for analysis of biochemical markers. Then, the rats were sacrificed by cervical dislocation and the livers were harvested carefully, thoroughly washed in isotonic saline and blotted dry then, one portion of each liver was immediately snap-frozen in liquid nitrogen and stored at -80ºC for molecular evaluation. Other liver portion was preserved in formalin saline (10%) for histopathological procedure.

Biochemical analyses using ELISA

Rat vascular endothelial growth factor (VEGF) and the chemokine (C-C motif) ligand 2 (CCL2) [Angiogenesis markers], rat c-myc, p53 and caspase 8 (CAS8) [Apoptosis markers], rat S100 β ,calcium-binding protein β, (S100β) [Metastatic marker], rat zinc finger E-box binding homeobox 1 (Zeb1) [Epithelial-mesenchymal transition marker], and rat hepatic growth factor (HGF)[Hepatic growth marker] were quantified in serum using ELISA kits (Wuhan Fine Biotech, China) according to the

manufacturer's instructions.

Molecular genetic evaluation using quantitative real time qRT-PCR

The gene expression levels of VEGF, CCL2, c-myc, p53, Zeb1 and HGF were detected quantitavely using quantitative real time qRT-PCR. Total RNA were isolated from liver tissues of rats in all groups by the RNAeasy Mini extraction kit (Qiagen, Germany). The RNA integrity was assured with ethidium bromide stain analysis using agarose gel electrophoresis. Aliquots were used immediately for reverse transcription (RT). The complete poly(A)+ RNA isolated from each rat liver tissue was reverse transcribed into cDNA in a total volume of 20 ml using RvertAidcDNA synthesis kit (Invitrogen, Germany).

Real-time PCR cycler (DT-lite, Russia) was used to determine the rat cDNA copy number. PCR reactions were set up in 25 µL reaction mixtures containing 12.5 µL SYBR green master mixture (ThermoFisher, USA); 0.5µL 0.2 mM sense primer, 0.5 µL0.2 mM antisense primer, 6.5 µL distilled water and 5 µL of cDNA template. The reaction program was allocated to three steps. First step was at 95.0 ℃ for 3 min. Second step consisted of 40 cycles in which each cycle divided to three steps: (a) at 95.0 ℃ for 15 s; (b) at 55.0 – 60.0 ℃ for 30 s; and (c) at 72.0 ℃ for 30 s. The third step was consisted of 40 cycles, which started at 60.0 ℃ and then increased by about 0.5℃ every 10 s up to 95.0 ℃. At the end of each qRT-PCR, a melting curve analysis was performed at 95.0 ℃, then 55.0 – 60.0 ℃, then 95.0 ℃ to check the quality of the used primers. Primer sequences and the size of the produced amplicons of rat VEGF, CCL2, CCR2, c-myc, p53, Zeb1 and HGF versus GAPDH as a house keeping gene were generated using Primer3 Program and verified by NCBI/ Primer-BLAST [Primer sequences of the selected genes are illustrated in Table (1)].

Histopathological procedure

After fixation of liver samples in 10% formalin saline for twenty four hours, washing was done in tap water. Then serial dilutions of ethyl alcohol were used for dehydration. Liver specimens were cleared in xylene and embedded in paraffin wax at 56ºC in hot air oven for twenty four hours. Paraffin wax blocks were sectioned at 4 µm thickness by slidge microtome. The obtained tissue sections were collected on glass slides, deparaffinized, and stained using the Hematoxylin and Eosin (H&E) staining procedure. The histological sections were examined using an Olympus TM light microscope (Baker et al., 1998).

Statistical analysis

All assays were repeated three independent times (n=3). Comparisons between nano-formulations and their free counterparts versus controls were done using a two-tailed Student's t test, and the values of $P < 0.05$ were considered statistically significant.

Results

Characterization of nanoprototypes

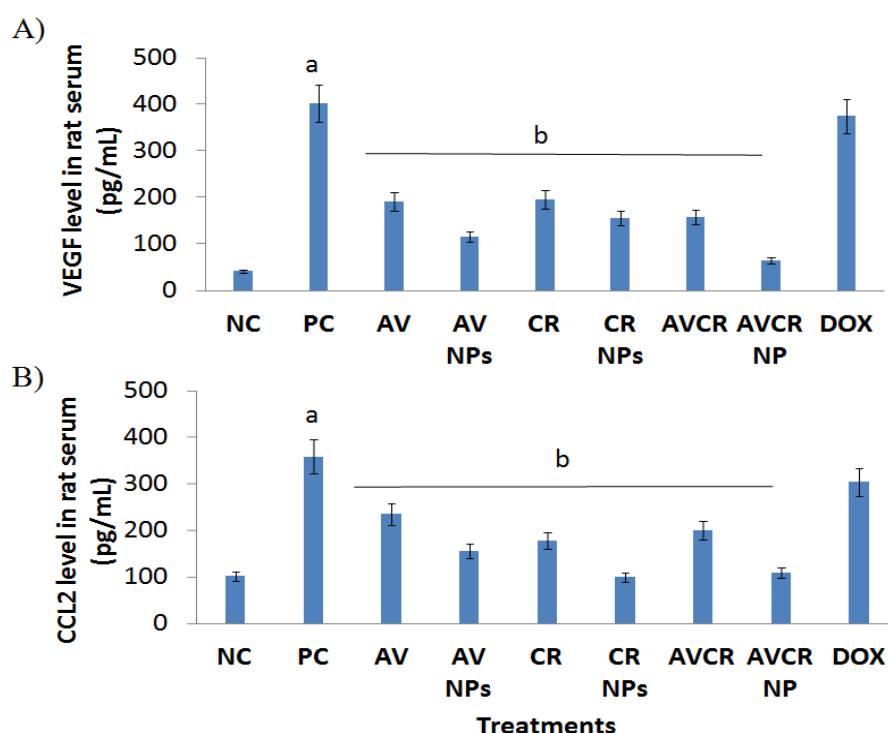The results of characterization of the designed

Figure 1. Serum Protein Levels of the Angiogenesis Markers (rat VEGF (A) and rat CCL2 (B) levels). These proteins levels were measured using ELISA. a, Significant change at $p< 0.05$ between the PC and NC groups; b, Significant change at $p< 0.05$ between the treated group and the PC group.

nanoprototypes were previously illustrated in our initial article (Abd-Rabou et al., 2019).

Biochemical and molecular genetics findings

The obtained data of serum levels of VEGF and CCL2 as angiogenesis markers in the negative control rats, HCC bearing rats (positive control rats) and in HCC bearing rats treated with AV, AVNPs, CR, CRNPs, AVCR, AVCRNPs and DOX are depicted in Fig. (1A and B). Also, the results of the gene expression levels of VEGF and CCL2 in the liver of the different studied groups are represented in Fig. (2). Our findings revealed that the affliction with HCC leads to significant enhancement (P<0.05) of VEGF and CCL2 serum levels along with significant up-regulation (P<0.05) of liver VEGF and CCL2 gene expression levels when compared with the negative control counterparts. Interestingly, all treatments except CR and DOX brought about significant reduction (P<0.05) in serum VEGF and CCL2 levels paralleled by significant down-regulation (P<0.05) in the gene expression levels of VEGF and CCL2 in the liver versus the positive controls. CR treatment in HCC-bearing rats induced significant reduction (P<0.05) in serum levels of VEGF and CCL2 in concomitant with significant down-regulation (P<0.05) in liver CCL2 gene expression level while, it produced insignificant down-regulation (P>0.05) in liver VEGF gene expression level in comparison with the positive control rats. Treatment with DOX in HCC-bearing rats caused insignificant change (P>0.05) in serum VEGF and CCL2 levels along with insignificant alteration (P>0.05) in liver VEGF and CCL2 gene expression levels in HCC rats contrary to the positive control rats. Importantly, we noticed that all AV-related regimens exhibited the most prominent effect

regarding the serum levels of VEGF and CCL2 and their gene expression levels in the liver.

The balance between the c-myc (the anti-apoptotic marker) and p53 (the pro-apoptotic marker) regarding the serological level or the tissue gene expression level was measured in the different studied groups as illustrated in

Table 1. Primer Sequences and the Size of the Produced Amplicons

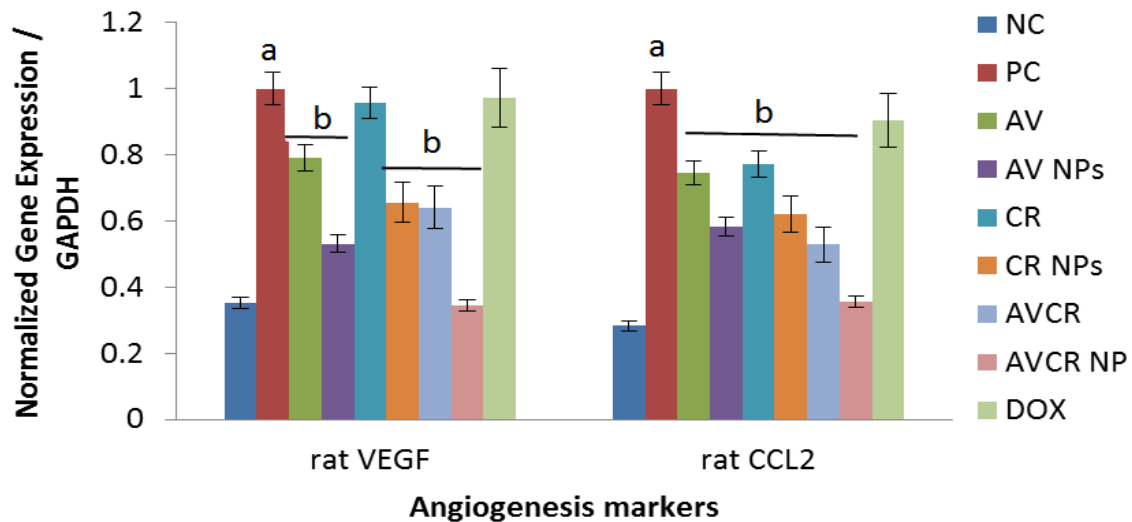| Genes	Primers	Product
Angiogenesis		
rat VEGF	F: 5′-CTC TTT TCT CTG CCT CCA TGA-3'	136 bp
	R: 5′-CCA TTG AAA CCA CTA ATT CTG TCC-3′	
rat CCL2	F: 5′-ATG CAG TTA ATG CCC CAC TC-3′	167 bp
	R: 5′-TTC CTT ATT GGG GTC AGC AC-3′	
rat CCR2	F: 5′-GAC CGA GTG AGC TCA ACA TTT-3′	159 bp
	R: 5′-AAC CCA ACT GAG ACT TCT TGC-3'	
Apoptosis		
rat c-myc	F: 5′-AAC TTA CAA TCT GCG AGC CA-3'	342 bp
	R: 5′- AGC AGC TCG AAT TTC TTC CAG ATA T-3′	
rat p53	F 5′- TTC CCT CAA TAA GCT GTT CTG CC-3′	538 bp
	R 5′- TGC TCT CTT TGC ACT CCC TGG-3'	
EMT genes		
rat Zeb1	F: 5′-TAG CCT TAA GGA AGC AGC CA-3'	218 bp
	R: 5′-TTA AGG CCA AAG GGA CAC AG-3'	
Growth factors genes		
rat HGF	F: 5′-TACACTCTTGACCCT GACACCC-3′,	378 bp
	R: 5′-TTTCCCATTGCCACGATA ACA-3′	
rat GAPDH	F: 5'-CCTGCACCACCAACTGCTTAGC-3'	239bbp
	R: 5'-GCCAGTGAGCTTCCCGTTCAGC-3'	

Figure 2. Genetic Expression Levels of the Angiogenesis Markers (rat VEGF and rat CCL2) in the Liver. The real time qRT-PCR was performed (n=3) of these genes normalized with GAPDH as a house keeping gene. a, Significant change at p< 0.05 between the PC and NC groups; b, Significant change at p< 0.05 between the treated group and the PC group.

Figure (3A and B) and Figure (4). Significant elevation in serum level of c-myc (P<0.05) in concomitant with significant reduction in P53 serum level (P<0.05) in HCC bearing rats (positive control rats) was observed. Likewise, the gene expression level of liver c-myc showed significant (P<0.05) up-regulation paralleled with significant (P<0.05) down-regulation in liver P53 gene expression level in HCC bearing rats in comparison with the negative control rats. Importantly, all treatments induced significant (P<0.05) suppression of serum level of c-myc along with significant (P<0.05) down-regulation in liver c-myc gene expression level in comparison with the positive controls. Moreover, the applied treatments in the present approach caused significant enhancement (P<0.05) in P53 serum level accompanied with significant up-regulation (P<0.05) in liver P53 gene expression level compared to the positive controls.

Regarding the obtained results for the serum levels of S100β and CAS8 in the different studied groups Fig. (3C and D), the induction of HCC produced significant increase (P<0.05) in S100β serum level while it caused significant decrease (P<0.05) in serum level of CAS8 versus the negative controls. Intriguingly, serum level of S100β displayed significant regression (P<0.05) while CAS8 serum level exhibited significant rise (P<0.05) following the treatment of HCC bearing rats with the suggested treatments relative to the positive control rats. Of note, the treatment with AV and its related formulations yielded a superior effect on recovering the balance between the anti-apoptotic and pro-apoptotic indices in HCC rat model.

The epithelial-mesenchymal transition (EMT) member (Zeb1) intimately correlates with chronic inflammatory situation as in case of liver cancer, Thus, we analysed the serum and liver gene expression levels of Zeb1 in the different studied groups Fig. (5A) and Fig. (6). Serum level of Zeb1 disclosed significant rise (P<0.05) in HCC bearing rats. Similarly, the gene expression level of Zeb1 in the liver exhibited significant up-regulation (P<0.05) in HCC bearing rats contrary to the negative control rats. The suggested treatments except CR and DOX in the present study produced significant drop (P<0.05) in serum Zeb1 level in concomitant with significant down-regulation (P<0.05) in liver gene expression level of Zeb1 versus the positive controls.CR treatment in HCC-bearing rats induced significant reduction (P<0.05) in Zeb1 serum level while, it produced insignificant down-regulation (P>0.05) in liver Zeb1gene expression level in respect with the positive control rats. DOX treatment in HCC- bearing rats induced significant enhancement (P<0.05) in Zeb1 serum level paralleled to significant up-regulation (P<0.05) in zeb1 gene expression level in the liver.

On the serum pattern, the level of HGF showed significant enhancement (P<0.05) in HCC bearing rats. As well, the gene expression level of HGF in the liver revealed significant up-regulation (P<0.05) in HCC afflicted rats compared to the negative control rats. In contrast, all treatments except CR and DOX presented in the current investigation caused significant decline (P<0.05) in serum level of HGF paralleled to significant down-regulation (P<0.05) in the gene expression level of HGF in comparison with the positive controls (Figure 5B) and Figure (6). Treatment of HCC-bearing rats with CR brought about significant drop (P<0.05) in HGF serum level while, it caused insignificant down-regulation (P>0.05) in liver HGF gene expression level as compared to the positive controls. DOX treatment in HCC-bearing rats displayed insignificant change (P>0.05) in serum HGF level in concomitant with insignificant alteration (P>0.05) in liver HGF gene expression level when compared to the positive control rats.

Histopathological description
   The histological micrographs of liver tissue sections of
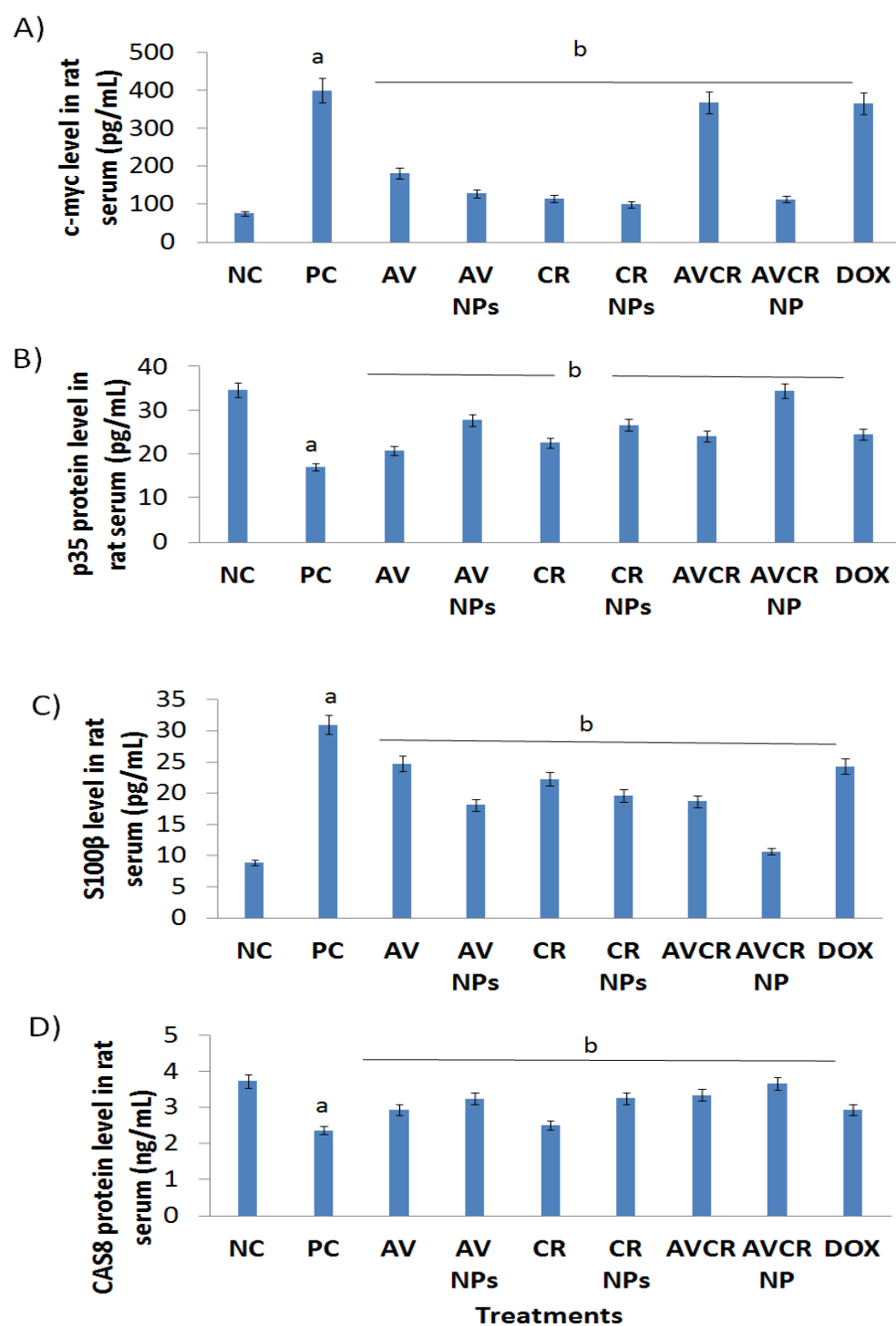
A)

B)

C)

D)

Figure 3. Serum Protein Levels of the Anti- Apoptotic Marker (rat c-myc (A)), pro-apoptotic marker (rat P53 (B)), (rat S100β (C)) and (rat CAS8 (D)). These protein levels were measured using ELISA. a, Significant change at p< 0.05 between the PC and NC groups; b, Significant change at p< 0.05 between the treated group and the PC group.

rats in the different experimental groups are represented in Figure (7). Figure (7A) illustrated the optical micrograph of liver tissue section of negative control rat showed no histopathological alteration in the liver and the normal histological structure of the liver was observed. The photograph of liver tissue section of rat bearing HCC induced by N-nitrosodiethylamine (NDEA) (positive control rat) revealed focal area of neoplastic cells in the parenchyma associated with inflammatory cells infiltration

in the portal area (Figure 7B). The liver's portal area of HCC bearing rat treated with AV showed inflammatory cells infiltration (Figure 7C). After treatment of HCC bearing rats with AVNPs, there was thickening and fibrosis appeared in the Glissons capsule (Figure 7D) associated with few inflammatory cells infiltration in the portal area of the liver (Figure 7E). The transverse section of liver of HCC- bearing rat treated with CR showed that the portal area has massive number of inflammatory
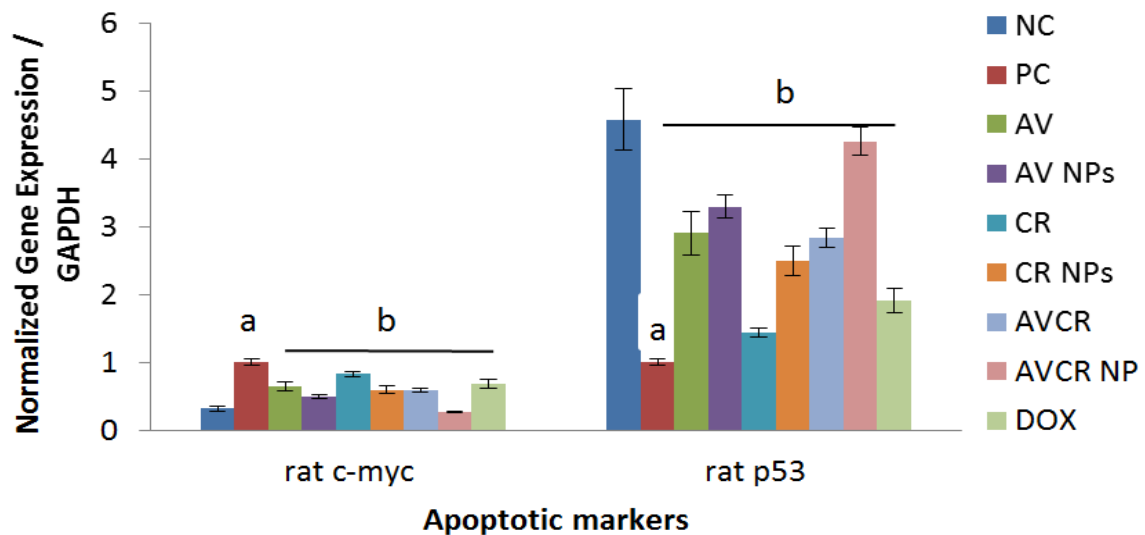
Figure 4. Genetic Expression Levels of the Anti- Apoptotic Marker (rat c-myc) and pro-apoptotic marker (rat p53) in the liver. The real time qRT-PCR was performed (n=3) of these genes normalized with GAPDH as a house keeping gene. a, Significant change at $p< 0.05$ between the PC and NC groups; b, Significant change at $p< 0.05$ between the treated group and the PC group.

cells infiltration (Figure 7F). Upon treatment of HCC-bearing rat with CRNPs, the Glissons capsule showed fibrosis and thickening (Figure 7G) associated with few inflammatory cells infiltration in the portal area of the liver (Figure 7H). Combinatorial therapy for HCC-bearing rat with AV and CR (AVCR) showed that the portal area has inflammatory cells infiltration and oedema with dilatation in the portal vein (Figure 7I). Intriguingly, the treatment of HCC bearing rat with AVCRNPs restored the liver histoarchitecture to the normal with no recorded

histopathological alteration (Figure 7J). Upon treatment of HCC bearing rat with DOX, the inflammatory cells infiltration was detected in the portal area in association with degeneration in focal hepatocytes in the hepatic parenchyma (Figure 7k).

Discussion

Hepatocellular carcinoma (HCC) appears to be amenable to immunotherapy and it has been reported
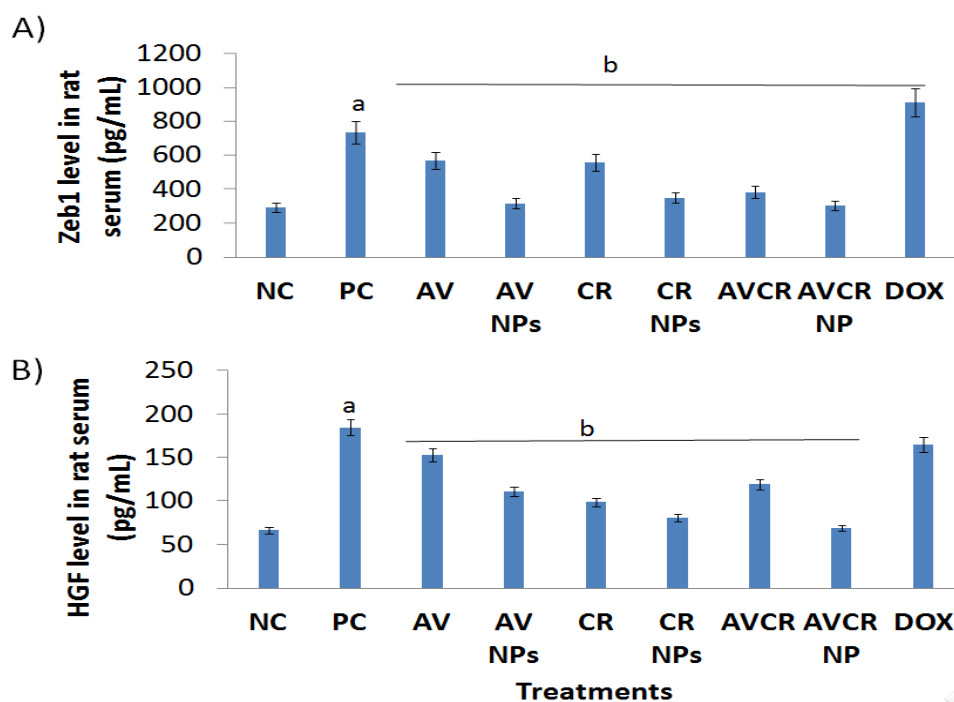

Figure 5. Serum Protein Levels of the EMT Marker (rat Zeb1) and Hepatic Growth Marker (rat HGF). These protein levels were measured using ELISA. a, Significant change at $p< 0.05$ between the PC and NC groups; b, Significant change at $p< 0.05$ between the treated group and the PC group.
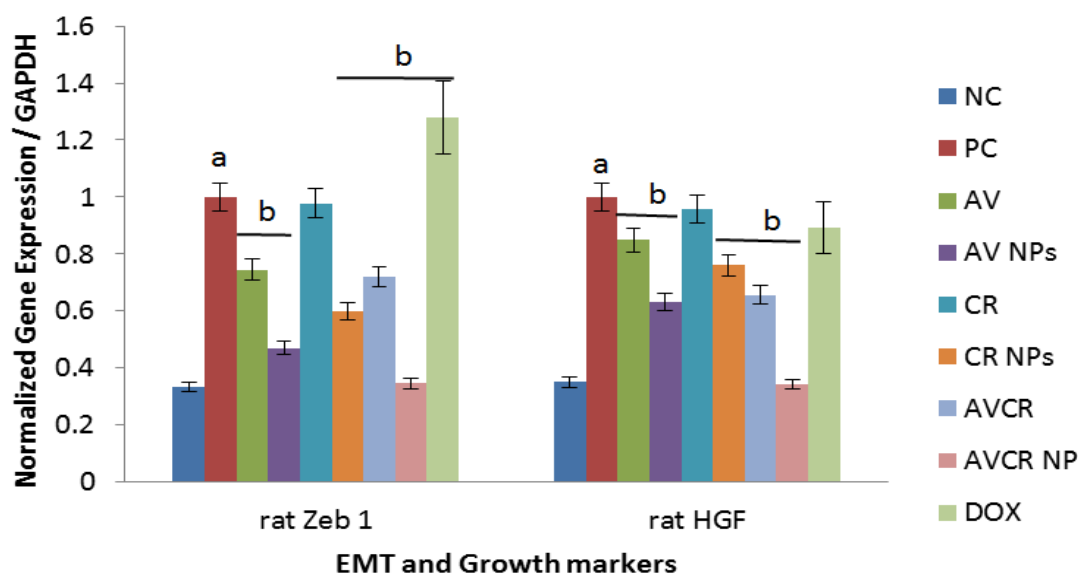
Figure 6. Genetic Expression Levels of the EMT Marker (rat Zeb1) and Hepatic Growth Marker (rat HGF) in the Liver. The real time qRT-PCR was performed (n=3) of these genes normalized with GAPDH as a house keeping gene. a, Significant change at $p< 0.05$ between the PC and NC groups; b, Significant change at $p< 0.05$ between the treated group and the PC group.
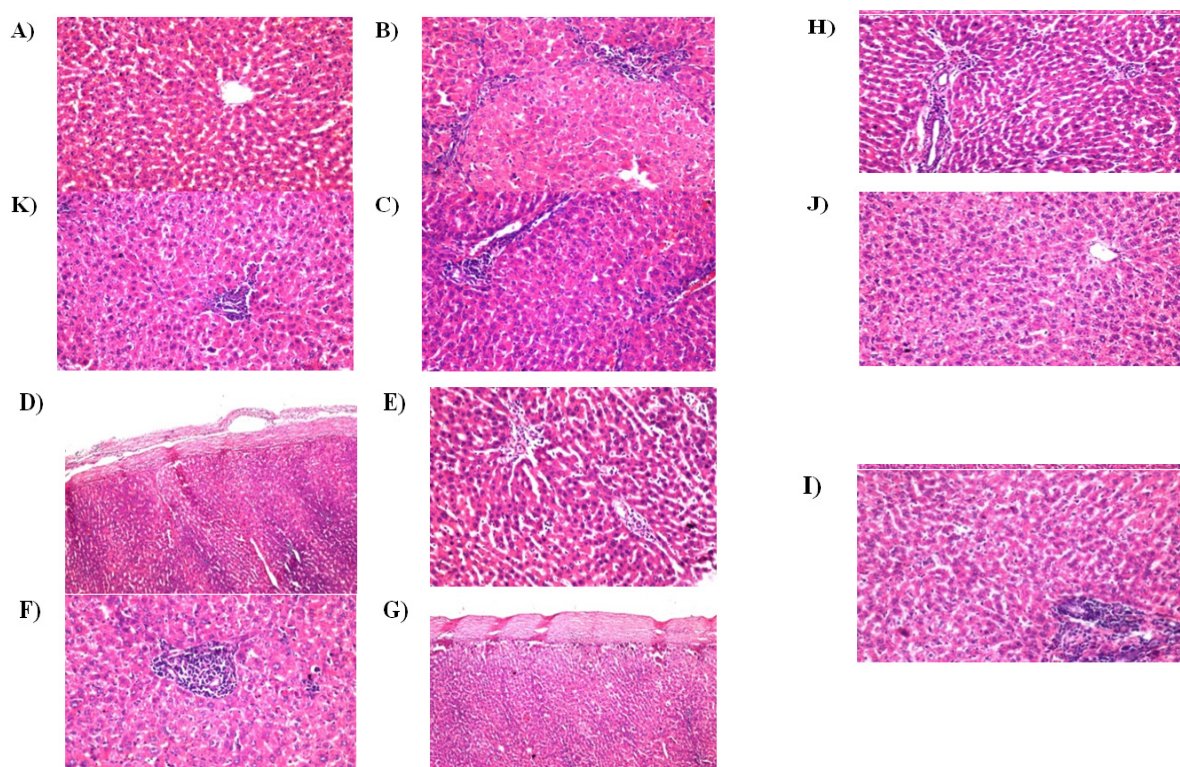

Figure 7. Histopathological Description of Liver Tissue Sections . A) Group of rats kept as negative control: There is no observed histopathological alteration and the normal histological structure is noticed. B) Goup of experimentally HCC induced rats (positive control): Focal area of neoplastic cells is observed in the parenchyma associated with inflammatory cells infiltration in the portal area. C) Group of experimentally HCC induced rats and treated with AV: The portal area shows inflammatory cells infiltration. D,E) Group of experimentally HCC induced rats and treated with AVNPs: There are thickening and fibrosis in the Glissons capsule (D) associated with few inflammatory cells infiltration in the portal area (E). F) Group of experimentally HCC induced rats and treated with CR: The portal area shows massive number of inflammatory cells infiltration. G, H) Group of experimentally HCC induced rats and treated with CRNPs: The Glissons capsule shows fibrosis and thickening (G) associated with few inflammatory cells infiltration in the portal area (H). I) Group of experimentally HCC induced rats and treated with AVCR: The portal area shows inflammatory cells infiltration and oedema with dilatation in the portal vein. J) Group of experimentally HCC induced rats and treated with AVCRNPs: There is no histopathological alteration has been noticed. K) Group of experimentally HCC induced rats and treated with DOX.: Inflammatory cells infiltration is detected in the portal area associated with degeneration in focal few hepatocytes in the hepatic parenchyma.

that the tumor microenvironment in hepatic tumor has an accumulation of intratumoral immune cells that have an enhanced expression of exhaustion markers. These cells are activated but are exhausted and are not able to elicit tumor cell killing in an effective way. The combining medications bring about a paradigm shift in the treatment of advanced HCC (Niu et al., 2021).

Nowadays, nanoformulations are known to significantly enhance the effect of certain compounds compared to their free formula (Ardekani et al., 2015) and the nanodelivery methods are usually incorporated into therapeutic regimen of multiple diseases, including cancer (Bertrand et al., 2014). The advantages of using polyethylene glycol (PEG) and poly-l-lysine (PLL) in the fabrication of AVNPs, CRNPs, and AVCRNPs are the hydro- and bio-degradability of these compounds as well as biocompatibility (Umano et al., 2011), so they are suitable as drug delivery carrier.

Antibodies can be conjugated on the surface of nanocarriers to improve the specificity of delivery to target tissues or specific cell antigens (Kumari et al., 2010; Sousa et al., 2016). AV in PLGA NPs (Sousa et al., 2017) retained *in vitro* anti-VEGF activity against human umbilical endothelial cells (HUVEC). This bioactivity of AV-loaded NPs was maintained for 6 months at different storage conditions (4, 25, and 40 ºC) (Sousa et al., 2018). AVNPs were cytotoxic against human non-small cell lung carcinoma cell line (A549) with a median inhibitory concentration (IC50) of 1.8 µM and higher internalization (3-fold) than in a normal lung fibroblast cell (MRC-5) (Srinivasan et al., 2013). AV-loaded PLA nanoparticles decreased survival of A549 cells and human breast cancer cells (MCF-7 and MDA-MB-231) cells (Ligiero et al., 2016). AV-loaded PLGA nanoparticles reduced more the tumor growth than the control group in a glioblastoma mice model with a decrease in the VEGF mRNA expression (Alves et al., 2021).

In the current study, we utilized our previous designed, manufactured and characterized AV, CR, AVCR nanoprototypes, in comparison with their free formula and DOX, based on the knowledge of cancer cell microenvironment, *in vivo* to understand the underlying mechanisms that may facilitate the development of novel anti-cancer therapies for HCC.

AV or AVNPs in the current setting, caused significant decline in serum VEGF level along with significant down-regulation in liver VEGF gene expression level in HCC bearing rats. AV is a recombinant humanized monoclonal IgG1 antibody that binds to human VEGF which is essential for both the normal cell and tumor cell angiogenesis (Li and Kroetz, 2018). The mechanism of AV action is based on the neutralization of VEGF, so, it is used as anti-angiogenic therapy (Sousa et al., 2017). The inhibition of the VEGF signaling pathway improves cytotoxic drugs delivery by lowering tumor interstitial fluid pressure and reducing the number of nonfunctional tumor blood vessels (Garcia et al., 2020).

In the current approach, DOX insignificantly reduced the serum level of VEGF as well as it insignificantly down-regulated the liver expression level of VEGF gene. Many data have suggested that the anti-cancer chemotherapeutic drugs may have suppressing effects on angiogenesis and tumor vasculature function (Sanz-Cameno et al., 2010).

AV or AVNPs in the present investigation displayed significant depletion in serum level of CCL2 in concomitant with significant down-regulation of liver CCL2 gene expression level. It has been reported that AV administration significantly decreases mRNA and protein levels of the pro-inflammatory cytokines IL-6, CCL2 and RANTES in HUVECs treated with lipopolysaccharide (LPS) (Jeong et al., 2013).

In the current research, DOX administration in HCC bearing rats induced insignificant reduction in serum CCL2 level paralleled by insignificant down-regulation in CCL2 gene expression level in the liver. Evans et al. (2022) demonstrated a significant increase in CCl2 (MCP-1) serum cytokine concentration at 24 h and a significant decrease at 1 week past DOX when compared to the 0- to 6 h time point. Comparing 24 h and 1 week post DOX, there was a significant decrease in CCL2 (MCP-1) cytokine concentrations in dogs with lymphoma. On the clinical level, the study of Hamed Anber et al., (2019) indicated that MCP-1 significantly decreases post chemotherapy in non- Hodgkin lymphoma (NHL) patients.

The obtained results in this study indicated significant reduction in serum level of c-myc associated with significant down-regulation of c-myc in the liver in AV or AVNPs-treated groups. The proto-oncogene c-myc was recently identified as a master regulator of angiogenic factors essential for the proper expression of many components of the angiogenic network, including both positive (VEGF and angiopoietin-2) and negative (thrombospondin-1) cytokines (Baudino et al., 2002). Interestingly, c-myc-induced VEGF expression was enhanced in conjunction with hypoxia (Knies-Bamforth et al., 2004), and a direct correlation between c-myc over-expression and high levels of VEGF was observed *in vivo* (Aref et al., 2004).

C-myc serum level as well as c-myc gene expression in the liver in the present approach displayed significant down-regulation upon treatment of HCC-bearing rats with CR or CRNPs. Silencing CCR2 in dormant human colorectal adenocarcinoma cell line (HT29) resulted in the reduction of c-myc (Ren et al., 2021). Activated STAT3 signaling can regulate a variety of downstream targetgenes such as VEGF, Bcl-Xl, c-myc, and cyclin D1 to induce angiogenesis, inhibit apoptosis and promote cell proliferation (Yuan et al., 2015). Thus targeting the CCL2-CCR2 axis by blocking the receptor or the ligand could be an effective HCC therapy (Teng et al., 2017).

Our *in vivo* outcomes indicated that AV or AVNPs sensitized cancerous tissues. This sensitization is approached by cytotoxicity-mediated apoptosis through elevation of serum p53 level and up-regulation of p53 gene expression level in the liver of HCC-bearing rats to induce apoptosis in cancer cells (Mohammad et al., 2011). Induction of apoptosis by endoplasmic reticulum (ER) stress is implicated as the major factor in the development of multiple diseases. Thus, the anti-tumor effect of AV can be fulfilled on cellular level without depending on the forma¬tion of tumor vessel on tissue level. It was also observed that the expression of the p53 gene is increased

in myeloma cells influenced by AV-loaded chitosan NPs (Yousefi et al., 2021).

In the current investigation, DOX administration resulted in significant elevation in serum p53 level paralleled by significant up-regulation in liver p53 gene expression level in HCC-bearing rats. These findings are in accordance with the results of Wang et al. (2004) who reported that DOX causes early activation of p53 in tumor cells that is followed by caspase-3 activation and DNA fragmentation. Activation of p53, which in turn promotes apoptosis of tumor cells, is considered to be a key mechanism of action of antitumor drugs, including DOX (Lowe et al., 1994; Lotem et al., 1996).

In the current investigation, the administration of CR or CRNPs in HCC-bearing rats led to significant decline in serum S100β (Mantovani and Sica, 2010). Several studies indicated that, in the tumor microenvironment, TAMs acquire an M2-polarized phenotype and promote angiogenesis, metastasis, and suppression of adaptive immunity through the expression of cytokines, chemokines, growth factors, and matrix metalloproteases (Capece et al., 2013). These results demonstrated the translational potential of CCL2/CCR2 blockade for treatment of HCC (Li et al., 2017). S100β over-expression in gliomas enhanced TAM infiltration and promoted tumor growth *in vivo*. Additionally, S100β up-regulation resulted in increased angiogenesis and C-C motif ligand 2 (CCL2) over-expression. A positive correlation between S100β and CCL2 expression in human pro-neural and neural glioma subtypes has been reported (Wang et al., 2013).

Caspase 8 (CAS 8) serum level showed significant increase in HCC-bearing rats treated with AV or AVNPs in the present attempt. Caspases are members of a family of cysteine proteases that are divided into initiator caspases, such as CAS 8 and 9 and executioner caspases such as CAS 3 or 7 (Kumar, 1999). Initiator CAS 8 is known to be activated through extrinsic pathway, whereas CAS 9 is activated in the event of mitochondrial cytochrome c leakage (Ouyang et al., 2012). Induction of apoptosis in tumor cells specifically within the complex tumor microenvironment is highly desirable to kill them efficiently and to enhance the effects of chemotherapy. The study of Akal et al. (2015) demonstrated that the intra-cameral administration of AV in rats induces increased apoptotic activity represented by CAS 3 and CAS 8 staining in corneal tissue samples. Regarding the potency of AVNPs as an approach inducing apoptosis, Liao et al. (2015) found a complete tumor suppression with a great apoptotic index in the group of mice with liver cancer xenograft subjected to treatment with AV magnetic nanoparticles (Trejo-Solis et al., 2021).

DOX treatment in the present work caused significant enhancement of serum CAS 8 in serum of HCC-bearing rats. The alteration in Bcl-Xl (anti-apoptotic), Bax (pro-apoptotic) genes' expression, Bax /Bcl-Xl ratio and CAS 8 and 9 proteins' level following the stimulation of apoptosis by DOX in MCF-7 cells has been reported. CAS 8 levels in the MCF-7 cells exposed to DOX increased after 48 and 72 h incubation (Sharifi et al., 2015). DOX-induced apoptosis is regulated by the Bcl-2 family of proteins, upstream of caspase activation. The Bax gene expression

is known to cause the activation of caspases followed by apoptosis (Kagawa et al., 2000).

In the present attempt, treatment of HCC-bearing rats with AV or AVNPs induced significant inhibition of zinc finger E box binding homeobox 1 (ZEB-1) serum level paralleled to significant down-regulation in ZEB-1 gene expression level in the liver. As an activator of EMT, ZEB1, the member of zinc finger family, encodes the zinc finger and homeodomain transcription cytokine (Wang et al., 2009). Numerous studies have demonstrated that abnormal expression of ZEB1 in many types of liver disease including hepatitis, liver fibrosis, and hepatitis C virus (Kim et al., 2016; Li et al., 2019; Hu et al., 2020).

Currently, the treatment of HCC-bearing rats with AV or AVNPs produced significant drop in serum HGF level in concomitant with significant down-regulation in liver HGF gene expression level. This finding is consistent with the hypothesis that, in livers with a highly carcinogenic state and prevalent irregular regeneration, the increasing of the paracrine production and secretion of HGF from mesenchymal cells facilitate their regular regeneration of hepatocytes and thereby, promote the development of cancer (Yamagamim et al., 2002). It has been reported that low expression of HGF seems to be predictive of improved efficacy for AV treatment (Cloughesy et al., 2017).

The current histopathological observation revealed that the liver tissue section of rat bearing HCC induced by N-nitrosodiethylamine (NDEA) shows focal area of neoplastic cells in the parenchyma associated with inflammatory cells infiltration in the portal area. This finding comes in line with the study of Kartik et al. (2010) who demonstrated that NDEA induced HCC in rats that is evidenced by the arrangement of neoplastic cells in lobules separated by fibrous septa with inflammatory collection.

Therapeutic agents based on NPs targeting TAMs may represent a new approach to curing cancer in the clinic. Treatment of HCC-bearing rat with a combinatorial therapy of AV and CR (AVCR) showed that the portal area has inflammatory cells infiltration and edema with dilatation in the portal vein. In this context, we proposed that the synergism between the effect of AV as an effective and tolerable anti-liver cancer treatment and the effect of CR as effective enhancer of the tumor immunosuppressive environment leads to the appearance of this histological feature of the liver. The histopathological examination of liver tissue section of HCC- bearing rat treated with AVCRNPs showed the restoration of the liver histoarchitecture to the normal with no recorded histopathological alteration. This finding could be explained by the inhibition of liver cancer cell proliferation which is mediated by early apoptosis upon using nano-combination of CR with AV (Abd Rabou and Ahmed, 2019). Histopathological examination of liver tissue section of HCC-bearing rat treated with DOX revealed the inflammatory cells infiltration in the portal area in association with degeneration in focal hepatocytes in the hepatic parenchyma.

In conclusion, the anti-angiogenic treatment remains the backbone of systemic therapy for HCC. Also, the inhibition of CCR2 exhibits a substantial promise in

enhancing immunogenicity against this malignant disease. Here in, we have uncovered a new therapeutic strategy for targeting angiogenesis and blocking CCl2/CCR2 axis by CCR2 antagonist either in free state or nanoparticles formulation and also either individually or in combination in pre-clinical setting comprising HCC animal model. A multifaceted approach that employs anti-angiogenic therapy in combination with CCl2/CCR2 targeted immunotherapy enhances the therapeutic efficacy of the anti-angiogenic therapy and leads to reinforced potency compared to either agent alone in alleviating HCC. This supports the hypothesis that the anti-angiogenic drug when delivered in conjunction with CCR2 antagonism may be available modality for the treatment of HCC. Also, nanoencapsulation of monoclonal antibodies (avastin) is considered as an alternative to the current antibody based therapy, changing the route of administrations through controlled release of monoclonal antibodies and maintaining their stability and physicochemical characteristics. Moreover, the delivery of avastin in nanoscale delivery system provides more efficient tumor suppression as this way of transporting the drug intensifies drug local concentrations more efficiently. Additionally, targeting the tumor-associated immune cells by CCR2 antagonist in nanoscale with suitable physicochemical characteristics offers a potent and promising approach for HCC therapy. Furthermore, the outcomes of combinatorial therapy of nanoavastin with nano CCR2 inhibitor in the treatment of HCC murine model provide strong pre-clinical rationale for further clinical exploration of combining nanoparticles of anti-angiogenesis with CCR2 antagonism-directed immunotherapies in the treatment of HCC. This could be a novel possible therapeutic policy to supress tumor cell growth, survival, migration and consequently to terminate HCC.

Author Contribution Statement

All authors contributed in this work. AAA originated the research concept, synthesized and characterized the nanoparticles, performed the genetic experiments, and participated in biochemical and histo analyses, as well as graphical analysis, manuscript writing, and publication. HHA, SHM, SEK, and MSK contributed in animal modeling, biochemical and histo analyses, as well as manuscript editing.

Acknowledgements

Availability of data
    available upon request and approval of the authors.

Conflict of interest
    No conflict of interest between authors.

References

A.O.A.C (1995). Official Methods of Analysis, 16th ed, Association of Official Analysis, Washington, DC.

Abd-Rabou AA, A Zoheir KhM, Kishta MS, et al (2016). Nano-micelle of Moringa Oleifera seed oil triggers mitochondrial cancer cell apoptosis. *Asian Pac J Cancer Prev*, **17**, 4929-33.

Abd-Rabou AA, Ahmed HH (2019). Bevacizumab and CCR2 inhibitor nanoparticles induce cytotoxicity-mediated apoptosis in doxorubicin-treated hepatic and non-small lung cancer cells. *Asian Pac J Cancer Prev*, **20**, 2225-38.

Aglan HA, Ahmed HH, El-Toumy SA, Mahmoud NS (2017). Gallic acid against hepatocellular carcinoma: An integrated scheme of the potential mechanisms of action from *in vivo* study. *Tumour Biol*, **39**, 1010428317699127.

Akshatha GM, Raval SK, Arpitha GM, Raval SH, Ghodasara DJ (2018). Immunohistochemical, histopathological study and chemoprotective effect of Solanum nigrum in N-nitrosodiethylamine-induced hepatocellular carcinoma in Wistar rats. *Vet World*, **11**, 402-9.

Alves ACS , Bruinsmann FA, Guterres SS, Pohlmann AR. (2021). Organic nanocarriers for bevacizumab delivery: An Overview of Development, Characterization and Applications. *Molecules*, **26**, 4127.

Alzamzamy A, Elsayed H, Abd Elraouf M, Eltoukhy H, Megahed T, Aboubakr A (2021). Serum vascular endothelial growth factor as a tumor marker for hepatocellular carcinoma in hepatitis C virus-related cirrhotic patients. *World J Gastrointest Oncol*, **13**, 600-11.

Apte RS, Chen DS, Ferrara N (2019). VEGF in signaling and disease: beyond discovery and development. *Cell*, **176**, 1248–64.

Ardekani S, Scott HA, Gupta S, Eum S, Yang X, Brunelle AR (2015). Nanoliposomal nitroglycerin exerts potent anti-inflammatory effects. *Sci Rep*, **5**, 16258.

Aref S, Mabed M, Zalata K, Sakrana M, El Askalany H (2004). The interplay between c-Myc oncogene expression and circulating vascular endothelial growth factor (sVEGF), its antagonist receptor, soluble Flt-1 in diffuse large B cell lymphoma (DLBCL): relationship to patient outcome. *Leuk Lymphoma*, **45**, 499–506.

Baghban R, Roshangar L, Jahanban-Esfahlan R (2020). Tumor microenvironment complexity and therapeutic implications at a glance. *Cell Commun Signal*, **18**, 59.

Baker FJ, Silverton RE, Pallister CJ (1998). Introduction to laboratory technology. 7th Editon, Butterworth-Heinemann, Wobrun, MA, USA, ISBN-13: 978075621908; page 448.

Baudino TA, McKay C (2002). c-Myc is essential for vasculogenesis and angiogenesis during development and tumor progression. *Genes Dev*, **16**, 2530–43.

Bertrand N, Wu J, Xu X, Kamaly N, Farokhzad OC. (2014). Cancer nanotechnology: the impact of passive and active targeting in the era of modern cancer biology. *Adv Drug Deliv Rev*, **66**, 2–25.

Capece D, Fischietti M (2013). The inflammatory microenvironment in hepatocellular carcinoma: A Pivotal Role for Tumor-Associated Macrophages. Hindawi Publishing Corporation. *Biomed Res Int*, **2013**, 187204.

Cloughesy T, Finocchiaro G, Belda-Iniesta C, et al (2017). Randomized, double-blind, placebo-controlled, multicenter phase II study of on artuzumab plus bevacizumab versus

placebo plus bevacizumab in patients with recurrent glioblastoma: Efficacy, Safety, and Hepatocyte Growth Factor and O6-Methylguanine–DNA Methyltransferase Biomarker Analyses. *J Clin Oncol*, **35**, 343-50.

Conti I, Rollins BJ (2004). CCL2 (monocyte chemoattractant protein-1) and cancer. *Semin Cancer Biol*, **14**, 149- 54.

Evans BL, Fenger JM (2022). Serum IL-6 and MCP-1 concentrations in dogs with lymphoma before and after doxorubicin treatment as a potential marker of cellular senescence. *Vet Med Sci*, **8**, 85–96.

Fang WB, Jokar I, Zou A (2012a). CCL2/CCR2 chemokine signaling coordinates survival and motility of breast cancer cells through Smad3 protein-and p42/44 mitogen-activated protein kinase (MAPK)- dependent mechanisms. *J Biol Chem*, **287**, 36593- 608.

Farnsworth RH, Lackmann M, Achen MG, Stacker SA (2014). Vascular remodeling in cancer. *Oncogene*, **33**, 3496-505.

Fekry M, Mazrouaa AM, Mohamed MG, Kishta MS, Mansour NA (2021). The comparison between magnetite nanoparticles co-precipitated by different bases and their effects on human cells. *Int J Nanosci*, **20**, 2150021.

Ferrara N, Davis-Smyth T (1997). The biology of vascular endothelial growth factor. *Endocr Rev*, **18**, 4–25.

Fridlender ZG, Buchlis G, Kapoor V (2010). CCL2 blockade augments cancer immunotherapy. *Cancer Res*, **70**, 109–18.

Garcia J, Hurwitz HI, Sandler AB, et al (2020). Anti-tumour Treatment Bevacizumab (Avastin®) in cancer treatment: A review of 15 years of clinical experience and future outlook. *Cancer Treat Rev*, **86**, 102017.

Hamed Anber N , El-Sebaie A H , Darwish N H E, Mousa S A, Shamaa S S (2019). Prognostic value of some markers in patients with lymphoma. *Bioscience Rep*, **39**, BSR20182174.

Hernandez-Gea V, Tofanin S, Friedman SL, Llovet JM (2013). Role of the microenvironment in the pathogenesis and treatment of hepatocellular carcinoma. *Gastroenterology*, **144**, 512–27.

Hou XJ, Ye F, Li XY, Liu WT, Jing YY, Han ZP (2018). Immune response involved in liver damage and the activation of hepatic progenitor cells during liver tumorigenesis. *Cell Immunol*, **326**, 52–9

Hu S, Liu YM, Chen C, Li LY, Zhang BY, Yang JF (2020). MicroRNA-708 prevents ethanol-induced hepatic lipid accumulation and inflammatory reaction via direct targeting ZEB1. *Life Sci*, **258**, 118147.

Jeong SJ, Han SH, Kim CO, Choi JY, Kim JM (2013). Anti-vascular endothelial growth factor antibody attenuates inflammation and decreases mortality in an experimental model of severe sepsis. *Crit Care*, **17**, R97.

Kagawa S, Pearson SA (2000). A binary adenoviral vector system for expressing high levels of the proapoptotic gene bax. *Gene Ther*, **7**, 75-9.

Kartik R, Rao CV (2010). Exploring the protective effects of abrus precatorius in HepG2 and N-Nitrosodiethylamine-induced hepatocellular carcinoma in Swiss Albino rats. *Ranian J Pharmaceutical Sci Spring*, **6**, 99-114.

Kelley RK (2020). Atezolizumab plus bevacizumab-a landmark in liver cancer. *N Engl J Med*, **382**, 1953-55.

Kim JH, Lee CH, Lee SW (2016). Hepatitis C virus infection stimulates transforming growth factor-beta1 expression through up-regulating miR-192. *J Microbiol*, **54**, 520–6.

Knies-Bamforth UE, Fox SB, Poulsom R, Evan GI, Harris AL (2004). c-Myc interacts with hypoxia to induce angiogenesis *in vivo* by a vascular endothelial growth factor-dependent mechanism. *Cancer Res*, **64**, 6563–70.

Korbecki J, Kojder K, Simińska D, Bohatyrewicz R, Gutowska I, Chlubek D (2020). CC chemokines in a tumor: A Review of Pro-Cancer and Anti-Cancer Properties of the Ligands of Receptors CCR1, CCR2, CCR3, and CCR4. *Int J Mol Sci*, **21**, 8412.

Kumar S (1999). Regulation of caspase activation in apoptosis: implications in pathogenesis and treatment of disease. *Clin Exp Pharmacol Physiol*, **26**, 295-303.

Kumari A, Yadav S K, Yadav S C (2010). Biodegradable polymeric nanoparticles based drug delivery systems. *Colloids Surf B Biointerfaces*, **75**, 1–18.

Li LY, Yang CC (2019). ZEB1 regulates the activation of hepatic stellate cells through Wnt/beta-catenin signaling pathway. *Eur J Pharmacol*, **865**, 172787.

Li M, Kroetz D L (2018). Bevacizumab-induced Hypertension: Clinical Presentation and Molecular Understanding. *Pharmacol Ther,* **182**, 152–160.

Ligiero T B, Cerqueira-Coutinho C, Albernaz M S, et al (2016). Diagnosing gastrointestinal stromal tumours by single photon emission computed tomography using nano-radiopharmaceuticals based on bevacizumab monoclonal antibody. *Biomed Phys Eng Express*, **2**, 045017.

Lowe SW (1994). p53 status and the efficacy of cancer Therapy in Vivo. *Science*, **266**, 807–10.

Mantovani A, Sica A (2010). Macrophages, innate immunity and cancer: balance, tolerance, and diversity. *Curr Opin Immunol*, **22**, 231–7.

Matsui D, Nagai H, Mukozu T, Ogino YU, Sumino Y (2015). VEGF in patients with advanced hepatocellular carcinoma receiving intra-arterial chemotherapy. *Anticancer Res*, **35**, 2205-10.

Mohamed S H, Kotob S E, Ahmed H H, Abd-Rabou A A, Kishta M S (2019). Toxicological and histopathological *in vivo* studies for safe dose optimization of Avastin and CCR2 antagonist nanoparticles. *Biosci Res*, **16**, 596–619.

Mohammad R, Hasan SHYH, Owen DA, Tai IT (2011). Inhibition of VEGF induces cellular senescence in colorectal cancer cells. *Int J Cancer*, **129**, 2115–23.

Morvan MG, Lanier LL (2016). NK cells and cancer: you can teach innate cells new tricks. *Nat Rev Cancer*, **16**, 7-19.

Niu M, Yi M, Li N, Wu K, Wu K (2021). Advances of targeted therapy for hepatocellular carcinoma. *Front Oncol*, **11**, 719896.

Ouyang L, Shi Z (2012). Programmed cell death pathways in cancer: a review of apoptosis, autophagy and programmed necrosis. *Cell Prolif*, **45**, 487-98.

Park SC, Su D, Tello C (2012). Anti-VEGF therapy for the treatment of glaucoma: A focus on ranibizumab and bevacizumab. *Expert Opin Biol Ther*, **12**, 1641–7.

Qian BZ, Li J (2011). CCL2 recruits inflammatory monocytes to facilitate breast-tumour metastasis. *Nature*, **475**, 222–5.

Rahma OE, Hodi FS (2019). The intersection between tumor angiogenesis and immune suppression. *Clin Cancer Res*, **25**, 5449–57.

Ren X, Xiao J (2021). Inhibition of CCL7 derived from Mo-MDSCs prevents metastatic progression from latency in colorectal cancer. *Cell Death Dis*, **12**, 484.

Sanz-Cameno P, Trapero-Marugán M, Chaparro M (2010). Angiogenesis: from chronic liver inflammation to hepatocellular carcinoma. *J Oncol*, **27**, 21-7.

Sharifi S, Barar J (2015). Doxorubicin changes Bax /Bcl-xL ratio, caspase-8 and 9 in breast cancer cells. *Adv Pharm Bull*, **5**, 351-9

Shih T, Lindley C (2006). Bevacizumab: An angiogenesis inhibitor for the treatment of solid malignancies. *Clin Ther*, **28**, 1779–1802.

Sousa F, Castro P, Fonte P, et al (2017). A new paradigm for antiangiogenic therapy through controlled release of bevacizumab from PLGA nanoparticles. *Sci Rep*, **7**, 3736.

Sousa F, Cruz A, Pinto IM, Sarmento B (2016). Nanoparticles for

the delivery of therapeutic antibodies: Dogma or promising strategy?. *Expert Opin. Drug Deliv*, **14**, 1163–76.

Speiser DE, Ho PC, Verdeil G (2018). Nanoparticles provide long-term stability of bevacizumab preserving its antiangiogenic activity. *Acta Biomater*, **78**, 285–95.

Speiser DE, Ho PC, Verdeil G (2016). Regulatory circuits of T cell function in cancer. *Nat Rev Immunol*, **16**, 599-611.

Srinivasan AR, Lakshmikuttyamma A, Shoyele SA (2013). Investigation of the stability and cellular uptake of self-associated monoclonal antibody (MAb) nanoparticles by non-small lung cancer cells. *Mol Pharm*, **10**, 3275–84.

Swarna latha B (2020). Nano world in cancer therapy. *Asian Pac J Cancer Biol*, **5**, 183-8.

Teng KY, Han J, Zhang X, et al (2017). Blocking the CCL2-CCR2 axis using CCL2-neutralizing antibody is an effective therapy for hepatocellular cancer in a mouse model. *Mol Cancer Ther*, **16**, 312-22.

Tian Z, Hou X, Liu W, Han Z, Wei L (2017). Macrophages and hepatocellular carcinoma. *Cell Biosci*, **9**, 79.

Trejo-Solis C, Escamilla-Ramirez A (2021). Crosstalk of the Wnt/β catenin signaling pathway in the induction of apoptosis on cancer cells. *Pharmaceuticals*, **14**, 871.

TTsou P, Katayama H, Ostrin EJ, Hanash SM (2016). The emerging role of B cells in tumor immunity. *Cancer Res*, **76**, 5597-601.

Wang H, Zhang L, Zhang IY, et al (2013). S100B promotes glioma growth through chemoattraction of myeloid-derived macrophages. *Clin Cancer Res*, **19**, 3764-75.

Wang J, Lee S, Teh CE, et al (2009). The transcription repressor, ZEB1, cooperates with CtBP2 and HDAC1 to suppress IL-2 gene activation in T cells. *Int Immunol*, **21**, 227–35.

Wang S, Konorev EA (2004). Doxorubicin induces apoptosis in normal and tumor cells distinctly different mechanisms. *J Biol Chem*, **279**, 25535–43.

Wolf MJ, Hoos A, Bauer J, et al (2012). Endothelial CCR2 signaling induced by colon carcinoma cells enables extravasation via the JAK2-Stat5 and p38MAPK pathway. *Cancer Cell*, **22**, 91-105.

Yamagamim H, Moriyama M, Matsumura H, et al (2002). Serum concentrations of human hepatocyte growth factor is a useful indicator for predicting the occurrence of hepatocellular carcinomas in c-viral chronic liver diseases. *Cancer*, **95**, 824-34.

Ye W (2016). The complexity of translating anti-angiogenesis therapy from basic science to the clinic. *Dev Cell*, **37**, 114–25.

Yousefi Y, Mortezania Z, Abolmolouki M, Daemi A (2021). A novel form of anti-angiogenic molecular antibody drug induces apoptosis in myeloma cells after cultivation upon endothelial feeder cells. *Leuk Res,* **108**, 106617.

Yuan J, Zhang F, Niu R (2015). Multiple regulation pathways and pivotal biological functions of STAT3 in cancer. *Sci Rep*, **5**, 17663.

Zachariae CO, Anderson AO, Thompson HL (1990). Properties of monocyte chemotactic and activating factor (MCAF) purified from a human fibrosarcoma cell line. *J Exp Med*, **171**, 2177-82.

Zhang Y, Guo J, Zhang XL, et al (2015). Antibody fragment-armed mesoporous silica nanoparticles for the targeted 1 delivery of bevacizumab in ovarian cancer cells. *Int J Pharm*, **496**, 1026-33.